The role of wire imperfections in micro magnetic traps for atoms

Jérôme Estève, Christine Aussibal, Thorsten Schumm, Cristina Figl, Dominique Mailly, Isabelle Bouchoule, Christoph I Westbrook, Alain Aspect

The role of wire imperfections in micro magnetic traps for atoms

J. Estve[(1)], C. Aussibal[(1)], T. Schumm[(1)], C. Figl[(2)]
D. Mailly[(3)], I. Bouchoule[(1)], C. I. Westbrook[(1)] and A. Aspect[(1)]
[(1)] *Laboratoire Charles Fabry de l'Institut d'Optique, UMR 8501 du CNRS, 91403 Orsay, France*
[(2)] *Permanent address : Universität Hannover, D 30167 Hannover, Germany*
[(3)] *Laboratoire de Photonique et de Nanostructures, UPR 20 du CNRS, 91460 Marcoussis, France*

We present a quantitative study of roughness in the magnitude of the magnetic field produced by a current carrying microwire, *i.e.* in the trapping potential for paramagnetic atoms. We show that this potential roughness arises from deviations in the wire current flow due to geometric fluctuations of the edges of the wire : a measurement of the potential using cold trapped atoms agrees with the potential computed from the measurement of the wire edge roughness by a scanning electron microscope.

PACS numbers: 39.25.+k, 03.75.Be

Compared to using macroscopic structures, the use of microwires to produce trapping fields for atoms has many advantages and is very promising [1]. High magnetic field gradients and thus high confinements can be achieved as the atoms are brought close to the wires. Furthermore, a large variety of potentials may be designed including curved guides and beam splitters. The realization of strongly confining guides for atoms opens the possibility of single-mode guiding of the atoms. This enables one to consider the realization of a guided atom interferometer.

Several difficulties however are associated with the use of microwires. First, the proximity of the atoms to the metallic wires in which thermal currents are present introduces losses and heating of the atoms [1, 2, 3, 4, 5]. Second, a time independent longitudinal fragmentation of the atomic clouds at sufficiently low temperatures has been observed [2, 6, 7]. This fragmentation has been shown to be due to a potential roughness arising from distortions of the current flow inside the microwire [8]. The roughness decreases as the distance h from the wire increases [7] since fluctuations are averaged to zero when h is large compared to their wavelength. Rough potentials may be a problem for the realization of guided atom interferometry as they may introduce quantum reflection of guided atoms.

It has been proposed in Ref. [9] that the distortion of the current flow responsible for the potential roughness is due to geometric deformations of the wire edges. In this paper we show that this is indeed the case in our experimental situation. To this end, the potential roughness produced by a current carrying microwire is deduced from the measurements of the density distribution of an atomic cloud at thermal equilibrium for different heights above the wire. We also measure the wire roughness using a scanning electron microscope and we compute the expected potential roughness it induces. The result is found to be in good agreement with the measurement of the potential using the atoms.

The wires we use are produced using standard microelectronic techniques. A silicon wafer is first covered by a 200 nm silicon dioxide layer using thermal oxidation. Next, layers of titanium (20 nm) and gold (200 nm) are evaporated. The wire pattern is imprinted on a 6 μm thick photoresist by using optical lithography. Gold is electroplated between the resist walls using the first gold layer as an electrode. After removing the photoresist and the first gold and titanium layers, we obtain electroplated wires of thickness $u_0 = 4.5$ μm with a rectangular transverse profile (see Fig. 1). A planarizing dielectric layer (BCB, a benzocyclobutene-based polymer) is deposited to cover the central region of the chip. On top of the BCB, a 200 nm gold layer is evaporated to be used as an optical mirror for light at 780 nm. The distance between the center of the wire and the mirror layer has been measured to be 14(1) μm.

The magnetic trap is produced by a current I flowing through a Z-shaped microwire [10] together with an external uniform magnetic field $\mathbf{B_0}$ (along the y-axis, see Fig. 1) parallel to the chip surface and perpendicular to the central part of the wire. The central part of the Z-wire is 50 μm wide and 2800 μm long. Cold ^{87}Rb atoms, collected in a surface magneto-optical trap, are loaded into the magnetic trap after a stage of optical molasses and optical pumping to the $|F = 2, m = 2\rangle$ hyperfine state. The parameters for the initial trap are $I = 2$ A, $B_0 = 8$ G, $N_{\rm at} = 3 \times 10^6$ and $T = 50$ μK. The trap is then compressed ($I = 2$ A, $B_0 = 40$ G) so that efficient forced evaporative cooling can be applied. Finally, the trap is decompressed. Final values of I and B_0 vary from 200 mA to 300 mA and from 3 G to 14 G respectively so that the height of the magnetic trap above the wire ranges from 33 μm to 170 μm. An external longitudinal magnetic field of a few Gauss aligned along z is added to limit the strength of the transverse confinement and to avoid spin flip losses induced by technical noise. For these parameters, the trap is highly elongated along the z-axis. The transverse oscillation frequency is typically $\omega_\perp/(2\pi) = 3.5$ kHz and 120 Hz for traps at 33 μm and 170 μm from the wire respectively.

The potential roughness is deduced from measurements of the longitudinal density distribution of cold trapped atoms. The atomic density is probed using absorption

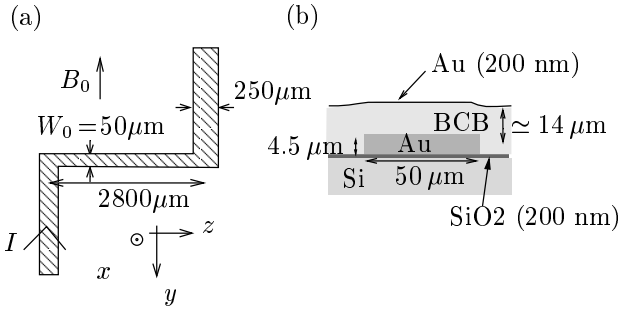

FIG. 1: (a) : Z-wire used to produce the magnetic trap. (b) : Cross section of the wire in the (xy) plane. The wire is covered with a layer of BCB polymer, and a thin gold layer acting as a mirror for the surface MOT and the absorption probe. The origin of the coordinate system is taken at the center of the wire.

imaging after the atoms have been released from the final trap by switching off the current in the Z-wire (switching time smaller than 100 μs). The probe beam is reflected by the chip at 45° allowing us to have two images of the cloud on the same picture. From images taken just after (500 μs) switching off the Z-wire current we infer the longitudinal density $n(z) = \int\int dxdy\, n(x,y,z)$. We also deduce the height of the atoms above the mirror layer from the distance between the two images. The temperature of the atoms is determined by measuring the expansion of the cloud in the transverse direction after longer times of flight (1 to 5 ms).

To infer the longitudinal potential experienced by the atoms, we assume the potential is given by

$$V(x,y,z) = V_z(z) + V_{\rm harm}(x,y) \qquad (1)$$

where $V_{\rm harm}(x,y)$ is a transverse harmonic potential. Under this separability assumption, the longitudinal potential is directly obtained from the measured longitudinal density of a cloud at thermal equilibrium using the Boltzmann law $V_z(z) = -k_{\rm B}T\ln(n(z))$. To maximise the sensitivity to the longitudinal potential variations, we choose a temperature of the same order as the variations ($T \simeq 0.4$ μK for traps at 170 μm from the wire and $T \simeq 2.2$ μK for traps at 33 μm from the wire). The separability assumption has been checked experimentally by deducing a z-dependent oscillation frequency from the rms width of the transverse atomic density at different positions. At 33 μm from the wire, there is no evidence of a varying oscillation frequency. At a height of 170 μm above the chip, over a longitudinal extent of 450 μm, we deduce a variation of the transverse oscillation frequency of about 13%. In this case, the assumption of separability introduces an error of $0.2\,k_{\rm B}T$ in the deduced potential.

The potential experienced by the atoms is $V = \mu_B|\vec{B}|$. To a very good approximation, the magnetic field at the minimum of $V_{\rm harm}$ is along the z-axis (for our parameters, the deviation from the z-axis is computed to be always smaller than 1 mrad) so that the longitudinal potential is given by $V_z(z) = \mu_B B_z(z)$. For a perfect Z-wire, the longitudinal potential is solely due to the arms of the wire and has a smooth shape. However, we observe a rough potential which is a signature for the presence of an additional spatially fluctuating longitudinal magnetic field. A spatially fluctuating transverse magnetic field of similar amplitude would give rise to transverse displacement of the potential which is undetectable with our imaging resolution and small enough to leave our analysis unchanged. In the following, we present the data analysis which enables us to extract the longitudinal potential roughness.

In order to have a large statistical sample and to gain access to low spatial frequencies, one must measure the potential roughness over a large fraction of the central wire. In our experiment, however, the longitudinal confinement produced by the arms of the Z-wire itself is too strong to enable the atomic cloud to spread over the full extent of the central wire. To circumvent this difficulty, we add an adjustable longitudinal gradient of B_z which shifts the atomic cloud along the central wire. We then measure the potential above different zones of the central wire. We typically use four different spatial zones which overlap each other by about 200 μm. We then reconstruct the potential over the total explored region by subtracting gradients from the potentials obtained in the different zones. Those gradients are chosen in order to minimize the difference between the potentials in the regions where they overlap.

We are interested in those potential variations which differ from the smooth confining potential due to the arms of the wire. We thus subtract the expected confining potential of an ideal wire from the reconstructed potential. To find the expected potential, we model the arms of the Z by two infinitesimally thin, semi-infinite wires of width 250 μm, separated by a distance l and assume a uniform current distribution. We fit each reconstructed potential to the sum of the result of the model and a gradient, using the gradient, l and the distance h above the wire as fitting parameters. The fitted values of l differ by a few percent from the nominal value 2.8 mm, while we find $h = 13(1)\,\mu$m+d where d is the distance from the mirror as measured in the trap images. This result is consistent with the measured 14 μm thickness of the BCB layer.

The potential which remains after the above subtraction procedure is plotted for different heights in Fig. 2. For a fixed trap height h (fixed ratio I/B_0), we have checked that the potential is proportional to the current in the wire; therefore we normalize all measurements to the wire current. The most obvious observation is that the amplitude of the roughness decreases as one gets further away from the wire. Furthermore fluctuations of small wavelength are washed out quickly as the distance to the wire increases. This is expected since fluctuations of wavelength much smaller than the height above the wire are averaged to zero. This is best seen in Fourier space. The spectral density of the potential roughness is shown in Fig. 3 for two different heights above the wire. We observe that the spectrum gets narrower as the

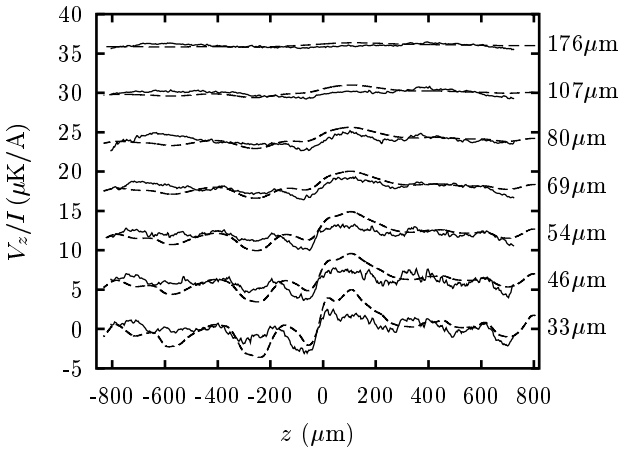

FIG. 2: Rough potentials normalized to the current in the Z-shaped wire for different heights from the wire. Solid lines : potentials measured using cold atomic clouds. Dashed lines : potentials calculated from the measured geometric roughness of the edges of the wire. The different curves have been shifted by 6 μK/A from each other and heights above the wire are indicated on the right.

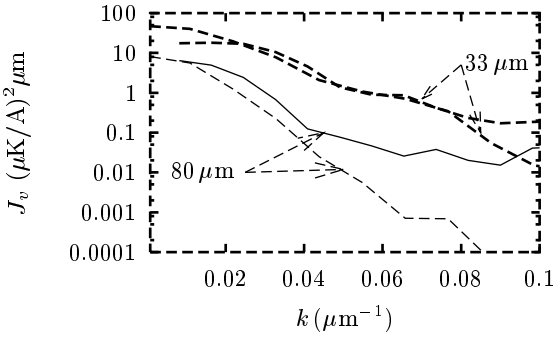

FIG. 3: Potential spectral density $J_v = 1/(2\pi I^2)\int_{-\infty}^{\infty}\langle V_z(z)V_z(z+u)\rangle e^{iku}du$ at 33 μm from the wire (fat lines) and at 80 μm from the wire (thin lines). Solid lines : potential measured using cold atomic clouds. Dashed lines : potentials calculated from the measured geometric fluctuations of the edges of the wire. These estimations of the spectral density are made with the Welch algorithm [11] using windows half the size of the total explored region (1.6 mm).

distance from the wire increases. At high wave vectors ($k > 0.07\,\mu\text{m}^{-1}$ at 33 μm and $k > 0.04\,\mu\text{m}^{-1}$ at 80 μm) we believe the spectrum is dominated by instrumental noise. Our use of the Boltzmann law to deduce the potential results in a scaling of the noise level by the temperature. Since the temperature used at 33 μm distance is about 4.6 times smaller than for clouds at 80 μm, we expect the noise level to be smaller by the same factor. This is consistent with the observation.

In the following we evaluate the rough potential due to edge fluctuations of the central wire. For this purpose, the edges of the wire are imaged using a scanning electron microscope (SEM), after removal of the BCB layer by reactive ion etching. Figure 4(a) indicates that the function f, which gives the deviation of the position of the wire edge from the mean position $y = \pm W_0/2$, is roughly independent of x. We make the approximation that f depends only on z. We deduce f from SEM images taken from above the wire (see Fig. 4(b)). To resolve f, whose rms amplitude is only 0.2 μm, we use fields of view as small as 50 μm. The function f is reconstructed over the entire length of the central wire using many images having about 18 μm overlaps. As shown in Fig. 4(c), several length scales appear in the spectrum. There are small fluctuations of correlation length of about 100 nm and, more importantly, fluctuations of larger wavelength (60 to 1000 μm).

The geometric fluctuations of the edges of the wire induce a distortion of the current flow which produces a longitudinal magnetic field roughness responsible for a potential roughness. To compute the current density in the wire, we assume a uniform resistivity inside the wire. We also assume that fluctuations are small enough to make the current density distortion linear in $f_{L/R}$, where $f_{L/R}$ are the fluctuations of the left and right edge of the wire respectively. The current density is in the yz-plane and, because the rough potential is proportional to the longitudinal magnetic field, we are only interested in its y component, j_y. Because of symmetry, only the part of $j_y(z,y)$ which is even in y contributes to B_z in the xz-plane. Thus, only the symmetric component $f^+ = 1/2(f_L + f_R)$ is considered. The Fourier component $f^+(k)$ of f^+ induces a transverse current density [9]

$$j_y^+(k,y) = ikf^+(k)\frac{I}{W_0 u_0}\frac{\cosh(ky)}{\cosh(kW_0/2)}. \qquad (2)$$

As the distances from the wire we consider (33 to 176 μm) are much larger than the thickness of the wire $u_0 = 4.5\,\mu$m we will in the following assume an infinitely flat wire. To efficiently compute the longitudinal magnetic field produced by these current distortions, we use the expansion on the modified Bessel functions of second kind $K_n(kx)$, which is valid for $x > W_0/2$. This expansion is, in the xz-plane,

$$B_z(k,x) = -\sum_{n\geq 0} k(c_{2n}(k) + c_{2n+2}(k))K_{2n+1}(kx) \qquad (3)$$

where

$$c_{2n}(k) = (-1)^n\frac{\mu_0}{\pi}u_0\int_0^{W_0/2} dy I_n(ky)j_y^+(k,y), \qquad (4)$$

I_n being the modified Bessel function of the first kind. For small wave numbers k such that $kW_0 \ll 1$, one expects the c_n coefficients to decrease rapidly with n. Indeed, for $kr \ll 1$, $I_n(kr) \simeq (kr)^n/(2^n n!)$. In our data analysis, only k wave vectors smaller than $0.07\,\mu\text{m}^{-1}$ are considered for which $kW_0/2 < 0.8$ so we expect the c_n coefficients to decrease rapidly with n. In the calculations, only the terms up to $n = 20$ are used.

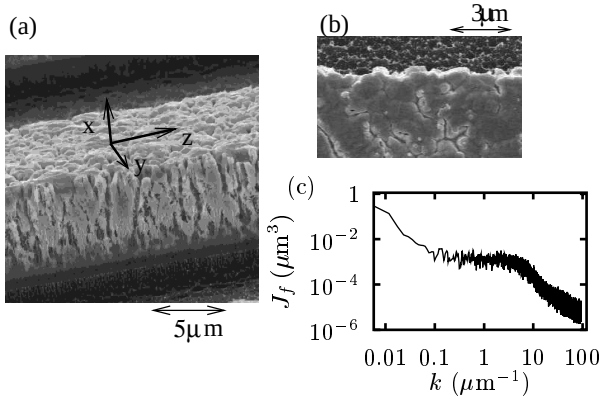

FIG. 4: Imperfections of the edges of the wire. In the SEM image of the wire taken from the side (a), one can see that the edge deviation function f is roughly independent of x. (c) Spectral density of f extracted from SEM images taken from the top as in Fig.(b).

Equations 2,4 and 3 then allow us to compute the fluctuating potential from the measured function f. In Fig. 3, we plot the spectral density of the potential roughness calculated from f for two different heights above the wire (33 and 80 μm) and compare it with those obtained from the potential measured with the atoms. For both heights, and for wave vectors small enough so that the measurements made with the atoms are not limited by experimental noise, the two curves are in good agreement. As we have measured the f function on the whole region explored by the atoms, we can compute directly the expected potential roughness. In Fig. 2, this calculated potential roughness is compared with the roughness measured with the atoms, for different heights above the wire. We find a good agreement between the curves. Remarkably the potential computed from the wire edges and the one deduced from the atomic distributions have not only consistent spectra but present well correlated profiles. We thus conclude that the potential roughness is due to the geometric fluctuations of the edges of the wire. The good agreement between the curves also validates the assumption of uniform conductivity inside the wire used to compute the current distortion flow.

As can be seen in Fig. 4, the top surface of the wire also presents some roughness. Using an atomic force microscope, we measure a rms fluctuation of 0.6 μm with a correlation length of 0.5 μm. Their calculated contribution to the rough potential gives a roughness spectral density at least one order of magnitude below the one measured with the atoms.

In conclusion, we have shown that the potential roughness that we observe can be attributed to the geometric fluctuations of the wire edges. Fluctuations at low wave vectors, responsible for the potential roughness, may be due to the lithography process. The magnetic field fluctuations are very small compared to the mean magnetic field due to the wire $\mu_0 I/2\pi h$ (6×10^{-4} in relative value at 33μm height from the wire). Thus, it is not surprising that small relative wire edge fluctuations ($f_{rms}/W_0 \simeq 10^{-3}$) explain the potential roughness. For a given wire technology, we expect the wire roughness to be independent on the wire width W_0. Assuming a white noise spectrum, the normalised potential roughness $V_{\rm rms}/I$ scales as $1/W_0^{5/2}$ for a fixed ratio h/W_0, h being the distance to the wire [9]. If one imposes an upper limit on the potential roughness, this scaling law will limit the minimum width of the wire and thus the maximum transverse confinement. To use smaller wires, a different fabrication process leading to smaller edges fluctuations has to be used. For example, electron beam lithography followed by gold evaporation may produce more straight wires.

Note that even for very straight edges, potential roughness may arise from other sources of current flow distortion such as bulk inhomogeneities.

We thank C. Henkel and H. Nguyen for helpfull discutions. This work was supported by E.U. (IST-2001-38863, HPRN-CT-2000-00125), by DGA (03.34.033) and by the french ministery of research (Action concerte ¡¡nanosciences-nanotechnologies¿¿).

[1] R. Folman *et al.*, Adv. Atom. Mol. Opt. Phys. **48**, 263 (2002), and references therein.
[2] J. Fortgh *et al.*, Phys. Rev. A **66**, 41604 (2002).
[3] M. P. A. Jones *et al.*, Phys. Rev. Lett. **91**, 80401 (2003).
[4] Y. Lin, I. Teper, C. Chin, and V. Vuletic, Phys. Rev. Lett. **92**, 050404 (2004).
[5] D. Harber, J. McGuirk, J. Obrecht, and E. Cornell, J. Low Temp. Phys. **133**, 229 (2003).
[6] A. E. Leanhardt *et al.*, Phys. Rev. Lett. **89**, 40401 (2002).
[7] M. P. A. Jones *et al.*, J. Phys. B: At. Mol. Opt. Phys. **37**, L15 (2004).
[8] S. Kraft *et al.*, J. Phys. B **35**, L469 (2002).
[9] D. Wang, M. Lukin, and E. Demler, cond-mat/0307402 (2003).
[10] J. Reichel, W. Hänsel, and T. W. Hänch, Phys. Rev. Lett. **83**, 3398 (1999).
[11] P. D. Welch, IEEE Trans. Audio and Electroacoustics **AU-15**, 70 (1967).